Saturation in the generation of THz signals with a contactless photoconductive antenna

Brian Grimaldi

(Dated: March 24, 2021)

Abstract

In this document, we study the effects of saturation in terahertz generation by using a pump-probe method. With this method, we vary the time delay between two ultra fast laser pulses and the fluence of the first laser pulse. We find that our expectations were met in the case of varying the fluence in the first pulse, however found that our findings in varying the time delay between pulses gave us the opposite results from what was expected. We were able to reconcile this by noticing that the timescale is different than our baseline expectation. These findings highlight the usefulness of using a photoconductive contactless antenna as a generation and material analysis platform.

I. INTRODUCTION

Terahertz (THz) radiation, defined on the electromagnetic spectrum in the frequency range of 0.1 - 10 THz [1], can be generated in several ways in the laboratory. One of the most common methods, developed in the late 1980's [2], involves electrically biased photoconductive (PC) antennas. These PC antennas are highly flexible platforms that can be tailored to various applications such as industrial [3], biological [4], and medical [5]. We can adjust the pump power, semiconductor generating material, the strength of the external electric field, and the frequency at which the antenna is operated to affect the emitted THz radiation. J.T Darrow [6] looked at how power scaled when using a large-aperture PC antenna, while K. Reiman looked at how small aperture PC antennas scaled the power down [1]. Research and comparison on the generation of THz using gallium arsenide (GaAs) and indium arsenide (InAs) have also been recorded for their different uses [7, 8]. In this work, we modify the traditional assembly of PC antennas by creating a gap between the electrodes and the semiconductor surface, substantially changing how the external electric field is created. We study how these new contactless PC antennas, when pumped by a Ti:Sapphire oscillator, compare to contacted PC antennas.

In a contacted PC antenna, metal electrodes are deposited directly on the surface of the semiconductor material to generate an external field that will initially separate the photogenerated carriers. By having the electrodes in contact with the surface, researchers are able to set the electric potential across a small region of the antenna, establishing an electric field. This method, while versatile, presents several significant drawbacks. Most semiconductor materials have a number of intrinsic carriers present even when not in contact by an external laser. These intrinsic carriers will flow between the electrodes, creating a dark current, which can lower the signal-to-noise ratio of the THz emitter. Additionally, this current contributes to power dissipation by the PC antenna, raising the temperature of the apparatus. As the temperature increases due to the dark current and to the laser hitting the surface, more intrinsic carriers are created, setting off a runaway process that results in thermal damage to the antenna. Another potential drawback to contacted antennas is that the electric field between the electrodes is not uniform. There is an interaction between the anode and the semiconductor that leads to a region of enhanced electric field near one electrode and a smaller field over the rest of the gap. If all that matters is generating a strong THz signal, this region of enhanced electric field can be useful. For other applications, however, it makes mod-

eling and understanding what is happening more difficult. Lastly, depositing the metal electrodes on the surface of the antenna is a non-trivial fabrication step that can impede testing of different generation media.

Contactless antennas do not suffer from the drawbacks of the contacted antenna. Since the electrodes are not in electrical contact with the semiconductor material, no current can flow between them. The external electric field is also uniform in the gap between the electrodes. We do not need to deposit metal on the surface of the antenna and create connections to the electrodes. However, there are a number of new drawbacks to the contactless antennas as well. First, the electric field experienced by the photogenerated carriers that creates the THz radiation is attenuated by an induced electric field due to intrinsic carriers responding to the external field. To minimize this effect, we need to change the direction of the external electric field across the gap at frequencies on the order of 100 MHz. This necessitates a custom-made power supply able to provide up to 40 W of power at radio frequencies. We are also limited to semiconductor materials with very low intrinsic carrier concentrations. Any material with a concentration larger than 100 times that of GaAs will result in little to no THz being generated in a contactless antenna.

Our goal in this work is to generate a large THz signal. In order to do this, we must pump a lot of energy into our system. This will create photogenerated carriers in the semiconductor material. We also must generate a large electric field for the photogenerated carriers to react to. This field will pull apart the electron-hole pairs and as a result of the speed at which they do so, generate a larger THz signal. Finally, we need to have a fast carrier response and small recombination time in our semiconductor. With these characteristics, we can delay the effects of thermalization and screening which would prevent new carriers from generating large THz signals.

In this paper, we will go over the theory behind the generation of THz radiation. We will also discuss induced electric field and Coulomb screening, and how these impedances must be overcome by a contactless antenna in order to prevent saturation in our THz generation. Next, we will go into depth on our experimental setup, explaining how the optical and electronic components work together to generate and analyze our THz signal. Finally, we will analyze and discuss our results from varying the intensity of the laser using the neutral density filter and the position on the second stage motor, creating a time delay between generating laser pulses.

II. THEORY

A. Antenna material

Semiconductors are the most common generation media for the generation of THz radiation. They are either single elements, such as silicon, or doped compounds, such as gallium arsenide. Metals and insulators have a valence band, where electrons reside when non-excited, a conduction band, that allows the electrons to move freely, and a band gap in between the valence and conduction band (see Fig. 1). The difference between a metal and an insulator is the value of the band gap. The band gap is devoid of energy levels, meaning an electron cannot exist within this region other than traveling through it to either the conduction or valance band. Insulators normally have very large band gaps, around 3 eV, while metals are much lower, allowing for the electrons to easily jump from the valance to conduction band. Gallium arsenide is a commonly used semiconductor when generating THz radiation. It has an energy gap of 1.43 eV, meaning a maximum wavelength of 867 nm is required to excite an electron to the conduction band [9]. Our broadband laser has a smaller central wavelength than the minimum wavelength of GaAs, therefore the maximum number of electrons we can strip from the valance band will be excited.

We want our GaAs sample to be as pure as possible, having as few intrinsic carriers present in the material as possibile. These intrinsic carriers tend to form during the formation of the semiconductor material, due to imperfections or environmental changes. Since there are usually imperfections in the making of GaAs, a very pure sample is hard to obtain. The purer the sample, the more resistive it is. This trait is very important as we want to try to minimize the amount of dark or induced current that is generated from electron excitation.

The GaAs sample that we use in our experiment has 10^6 intrinsic carriers per cm^3, unlike the average number for p-type or n-type which is $10^{16} - 10^{19} carriers/cm^3$. Silicon has an order of $10^{10} carriers/cm^3$ at room temperature. Out of all the options, GaAs has the lowest intrinsic carrier population, which will lead to a lower induced field in the presence of the external electric field.

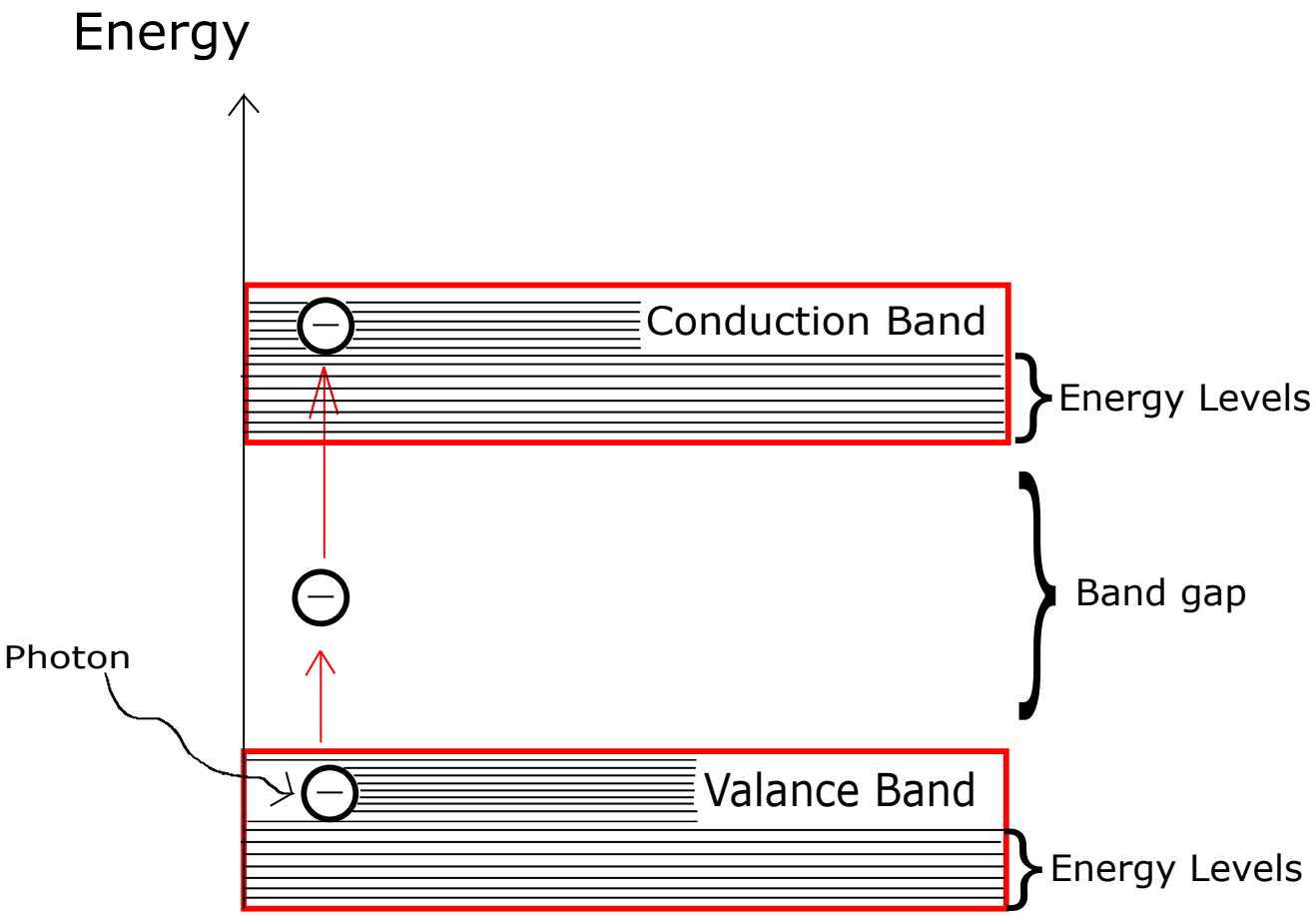

FIG. 1: Valance and Conduction band. Electron (minus sign) is excited by the incoming photon, jumping across a band gap until it is in the conduction band.

B. Generating THz from a photoconductive antenna

As shown in Fig. 2, when the laser light is absorbed by the GaAs, it creates a large population of photogenerated carriers within the area of the incident laser. These newly excited carriers begin to experience the external electric field generated by the contactless PC antenna, separating electrons and holes towards positive and negative electrodes, respectively. This separation creates an increasing induced field the farther apart these carriers are from one another. As the induced field becomes equal to or larger than external electric field, the carriers begin to slow down and accelerate in the opposite direction, causing them to move back towards each other. This process will repeat, making this motion look like an oscillating dipole. We can see this oscillating dipole in

the radiation of THz coming off of the antenna. As we can see in Fig. 3, THz waves are emanating in a dipole formation, polarized along the axis of the external electric field generated by the PC antenna. We then catch a small portion of this THz radiation, with the portion we are using polarized in the direction of the laser path (forward direction).

This oscillating dipole decreases in peak amplitude with time. This phenomenon is attributed to thermalization, or the Coulomb interactions between particles. Due to this thermalization and Coulomb interactions from other carriers (both intrinsic and excited), the excited carriers begin to slow down, eventually stopping oscillation together. This generally happens after 1 to 2 periods. These oscillations of electron-hole pairs due to the external electric field generate THz, where the THz signal is proportional to the amplitude of the oscillating field. The amplitude of the THz can increase due to more carriers moving through more excitation, a larger external field that increases the amplitude of oscillation of the charge population, and by using a material with a higher conductivity rate.

One thing to note regarding our THz signal is that because the laser excitation is much shorter compared to the THz pulse (50 femtoseconds vs 2 picoseconds), the THz electric field is phase locked to the laser repetition rate (see Fig. 4). When our laser pulse hits the semiconductor, we see it set in motion the generation of THz, where it oscillates across the horizontal axis where the vertical axis is the amplitude of the field. As a result, we know that the THz signal must be in phase with the laser repetition rate, assisting us in lock-in detection of THz signal.

C. Contactless vs contacted - Induced field vs applied voltage difference.

The external electric field is provided by a pair of straight metal electrodes. However, there is a difference between the how the carriers in a semiconductor experience the electric field. The first method is the contacted method, where the metal electrodes are deposited on the surface of the semiconductor. For this method, the carriers experience the electric field through direct contact. Since there is no induced field produced with this method, the power supply of the antenna does not need to be oscillated. However there is a dark current that flows through the electrodes, leading to thermal damage in the antenna and disrupting the signal to noise ratio.

Here, we are using a photo-conductive contactless antenna in our studies rather than a contacted antenna. The contactless antenna consists of a pair of metal electrodes that are electrically

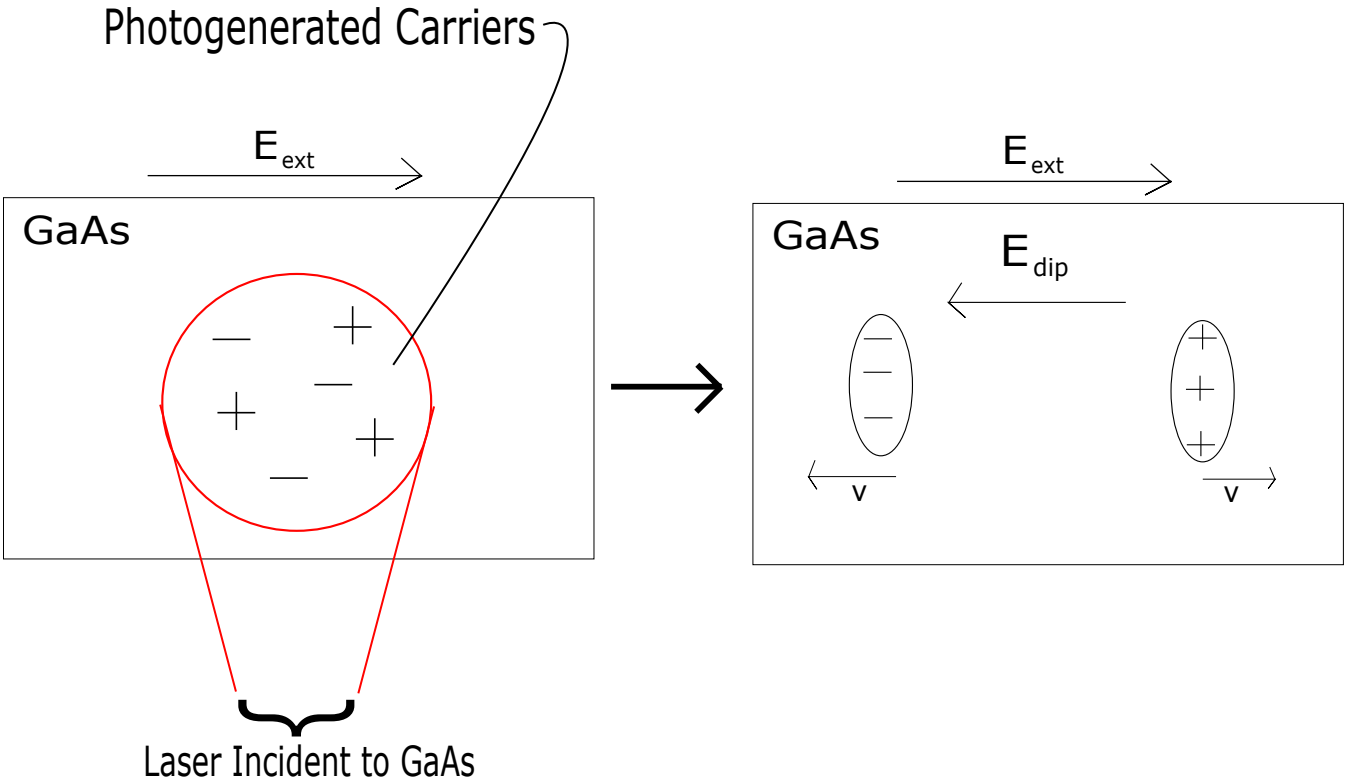

FIG. 2: Left hand side: Photogenerated carriers created due to laser incident to gallium arsenide (GaAs) sample. Right hand side: Electron-hole pair oscillation due to external electric field from contactless antenna. E_ext is the external electric field, E_dip is the induced electric field, GaAs is the gallium arsenide, + are holes, - are electrons, and v stands for the velocity.

insulated from the GaAs semiconductor, as opposed to being deposited on its surface. We use this experimental antenna to minimize the issue of thermal damage that is found within contacted antennas. The absence of dark current allows us to increase the power of the laser or increase the voltage across the antenna to study effects of saturation without damaging the antenna. However, there is an induced electric field generated by intrinsic carriers, differing from the aforementioned dark current. As a result, this large induced field will reduce the THz amplitude.

Fig. 5 illustrates how there are intrinsic carriers present in the GaAs before the laser is incident to its surface. There are many fewer carriers in the GaAs we use, having only 10^6 carriers/cm^3 compared to the average number of 10^{10} carriers/cm^3 for other semiconductor materials. When there is an applied external electric field on the excited material, for a contactless antenna, an induced field is generated from the electrons being attracted to the conducting end, and the holes

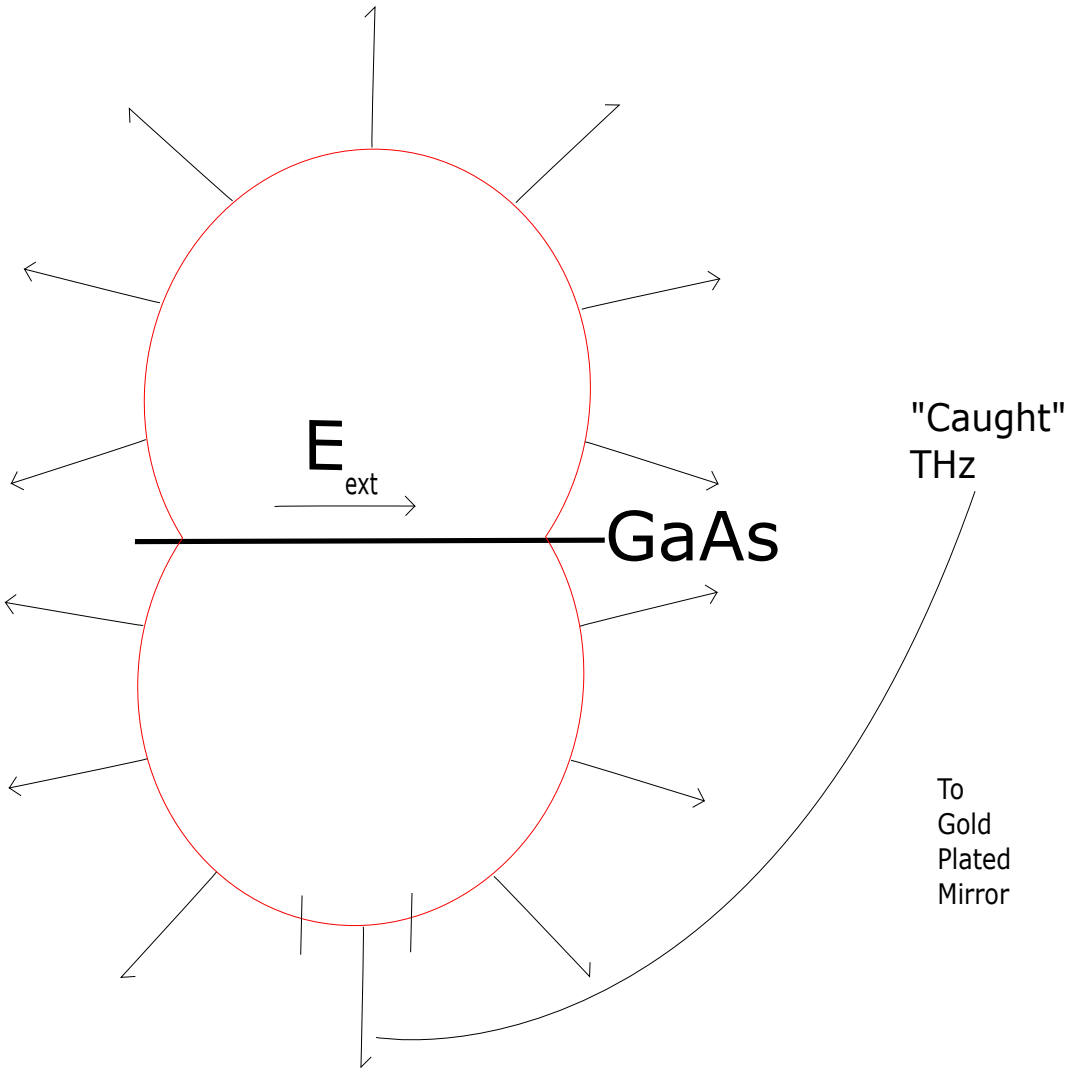

FIG. 3: Emanating THz from PC antenna. Partial red circles depict the dipole nature of the THz radiation, with arrows showing the direction an infinitesimal sliver is pointing in. Area captured between the two horizontal bars is the portion of THz that travels towards the gold plated elliptical mirrors.

moving towards the insulating end. We see that in Fig. 5, the induced electric field points in the opposite direction of the external field, sharply reducing the magnitude and, in turn, the intensity of the generated THz frequency. In order to prevent the induced field from building up too much, we alternate the direction of the external field at a frequency of 10 MHz.

We developed a MATLAB file to visualize the concept of how the external and induced electric

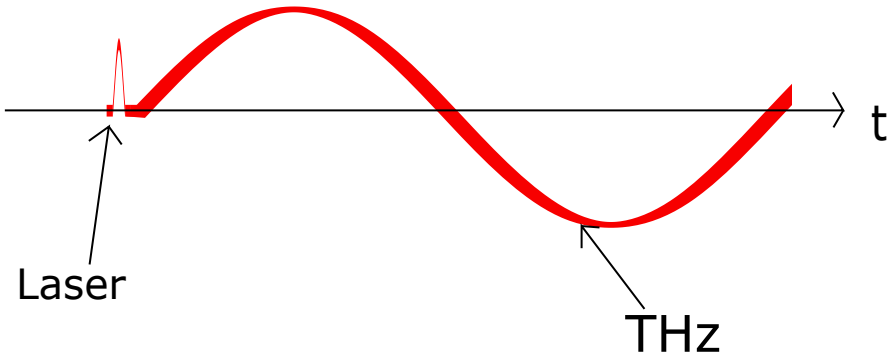

FIG. 4: Laser and THz signal compared to demonstrate time scale of the two. The laser has a very short time scale compared to the generated THz. The laser excites photogenerated carriers to create the upswing and downswing in THz generation that can be seen above. t stands for time on the horizontal axis. THz pulse is scaled appropriately, with respect to time, with the laser pulse to demonstrate size differences.

field affect the total field. As we can see in Appendix A, we begin by creating a step value to generate a time axis vector (range). Then, we define a value for the amplitude (amp). This amplitude will serve to signify the number of intrinsic carriers in the semiconductor material. The first function we generate is the external electric field (y) on line 6 of the code. This is a simple sinusoidal function, where the amplitude is the max electric field value. We can also adjust the frequency to produce varying results in our induced field. Our induced field (g) is then created using a for loop repeating for the amount of values in the external electric field vector. The loop has a base case to initialize the induced field and a normal case where it takes the previous value of the induced field and subtracts off the total electric field. This line of code allows the induced field to grow proportionally to the external electric field, where the larger the amp variable is, the larger the induced field will get. Finally, after the induced field has been accounted for in a loop, the total field (z) data index is generated through simple summation.

The results of this MATLAB code are shown in Fig. 6 and Fig. 7. In Fig. 6, the direction of the electric field is alternating slowly (top), with the induced field being able to effectively attenuate the total amplitude (middle and bottom, respectively). However, Fig. 7 shows that if we increase the frequency of the variation in the external field (top), the induced field (middle) will not have enough time to sharply attenuate the the total electric field (bottom).

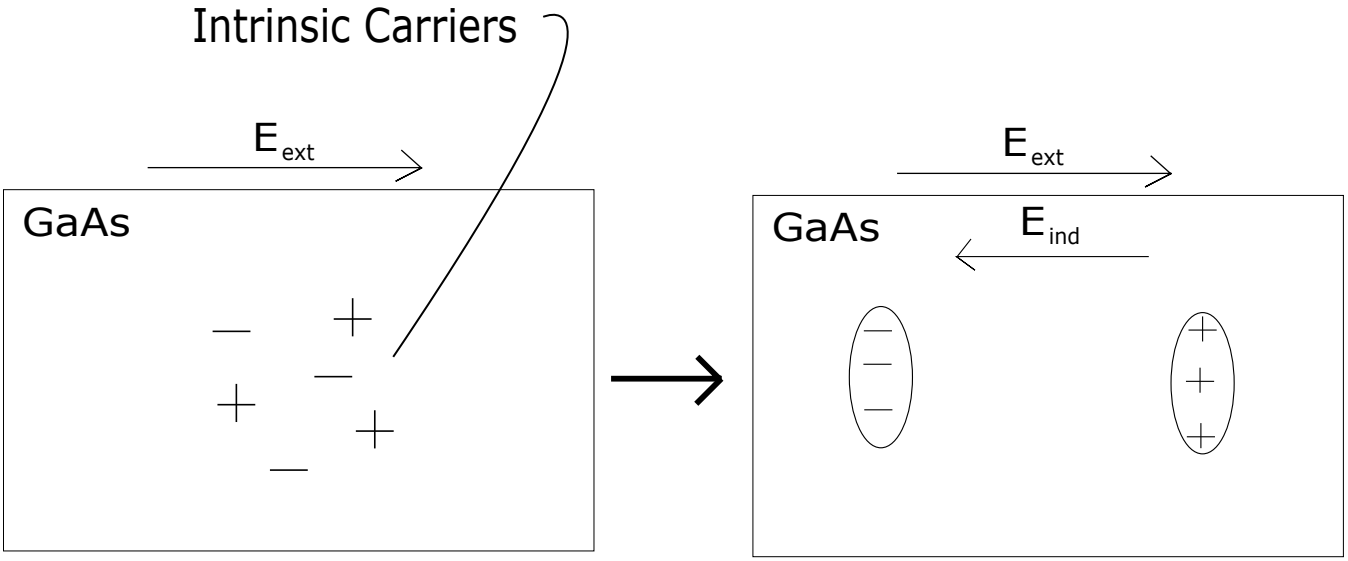

FIG. 5: Left hand side: Intrinsic carriers inherent in gallium arsenide (GaAs) sample due to imperfections in growing process. Right hand side: Electron-hole pair separation due to external electric field from contactless antenna. E_ext is the external electric field, E_ind is the induced electric field, GaAs is the gallium arsenide, + are holes, - are electrons.

Another way to slow the increase of the induced electric field over time is to have a very pure GaAs sample. With a purer sample, the resistivity of the GaAs is larger which means that when a laser is incident with the sample, electrons and holes will not be generated as fast as that of a not-as-pure sample. The reduction in the electron excitation over time will slow the increase of the induced field in the presence of a peak external field. We also reduced the amount of saturation in our THz generation by focusing our pulse train on the GaAs sample to cover as much of the semiconductor surface as possible. This creates a larger area for excited electron-hole pairs which will take longer for them to move to opposite ends of the surface when an external electric field is applied to the antenna.

The movement that the induced and photogenerated carriers experience is similar as they both react to the external field. The main difference between these two is the time scale. For reference, the time scale for the power supply is on the order of 10 nanoseconds (10^{-9}), the photogenerated carriers is 1 picosecond (10^{-12}), and the intrinsic carriers is about 1-100 nanoseconds. Due to the intrinsic carriers time scale being slightly larger than the power supply, it does not completely neutralize the external field. However, we are able to prevent this by alternating the power supply

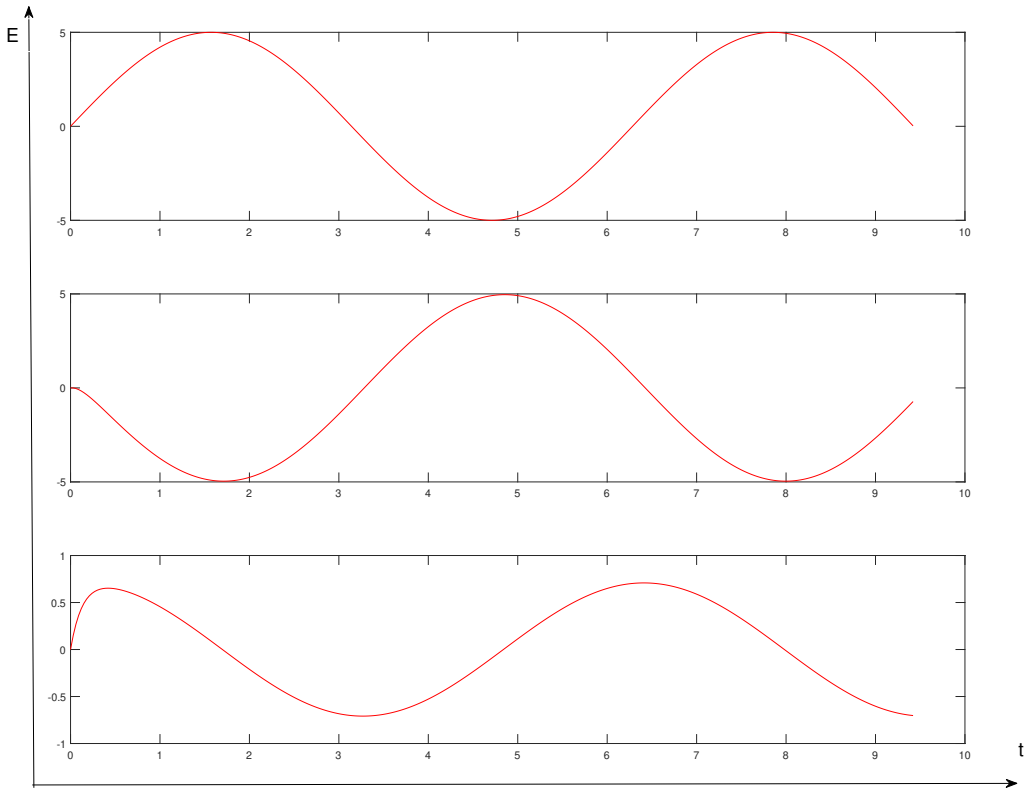

FIG. 6: External electric field (top graph) attenuated by the induced electric field (middle graph) to give a resulting total electric field (bottom). Horizontal axis represents time axis and vertical axis represents varying magnitudes in electric field.

to prevent a maximum attenuation. On the other hand, the time evolution of the photogenerated carriers is 10^{-4} times smaller than both the power supply and intrinsic carriers. This means that the total electric field will appear to be static when the photogenerated carriers begin to generate THz.

D. Coulomb screening

Coulomb screening is the phenomenon where a particular carrier (positive or negative in charge) experiences resistance due to multiple carriers. In Fig. 8, we can see a positive charge between positive and negative electrodes. In this case, we see there is nothing to impede the traveling

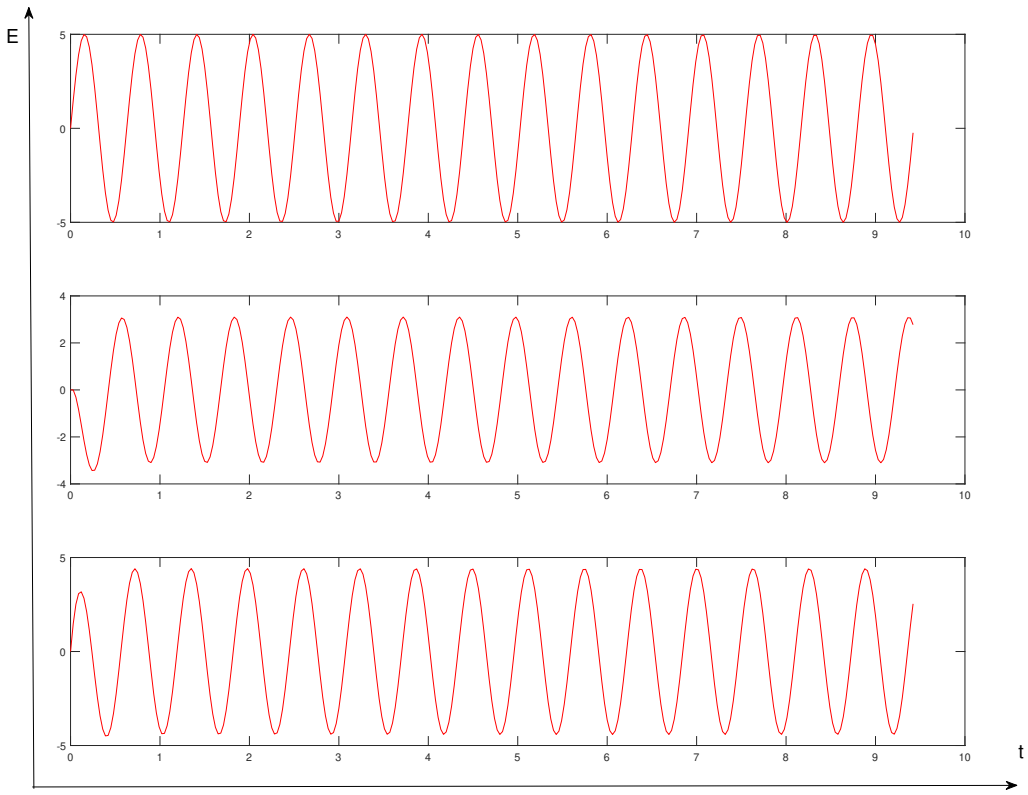

FIG. 7: External electric field (top graph) attenuated by the induced electric field (middle graph) to give a resulting total electric field (bottom). Horizontal axis represents time axis and vertical axis represents varying magnitudes in electric field. In this case, compared to the Fig. 5, frequency in external field is increased, slowing the increase of the induced electric field, resulting in a larger total electric field.

positive charge, allowing simple trajectory from one side to the other. However, in Fig. 9, we see Coulomb screening, where there are multiple charges in the center. As the charge moves through this system, its speed will be reduced by Coulomb interactions with the population of charges in the center.

Coulomb screening is integral to understanding how saturation occurs in THz generation with PC antennas. When the first pulse is incident on the GaAs, it creates a population of photogenerated carriers within the area of the focused beam. These photogenerated carriers from the first pulse will remain when the second pulse arrives at the GaAs. These additional carriers in the GaAs

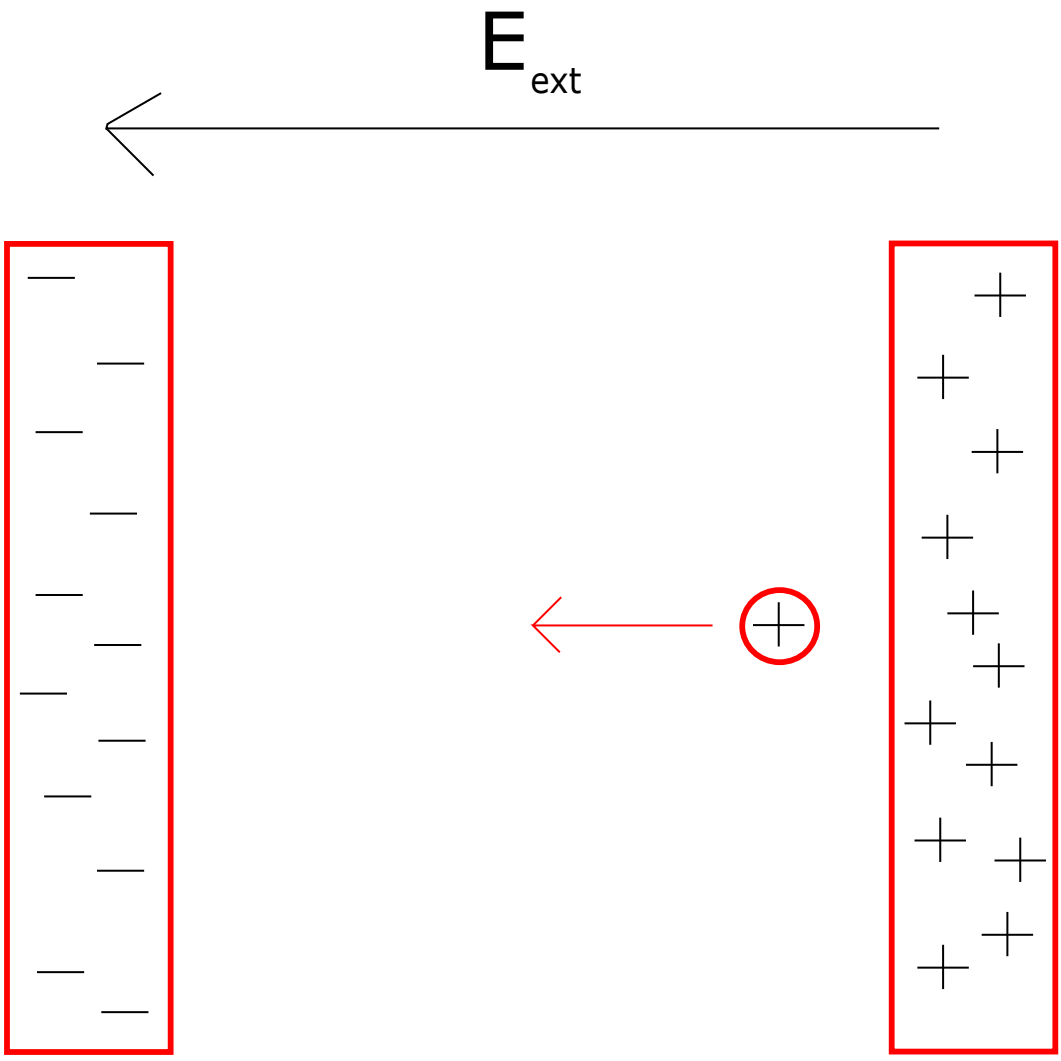

FIG. 8: Positive charge traveling in the direction of the electric field, uninhibited by other charges. Plus signs stand for positive charges and minus signs stand for negative charges.

will contribute to the Coulomb screening of the second pulse, therefore reducing the magnitude of the THz signal as a result. With even more carriers populating the semiconductor, the phenomenon depicted in Fig. 9 will be much greater, with more carriers inhibiting the path of the charge of interest.

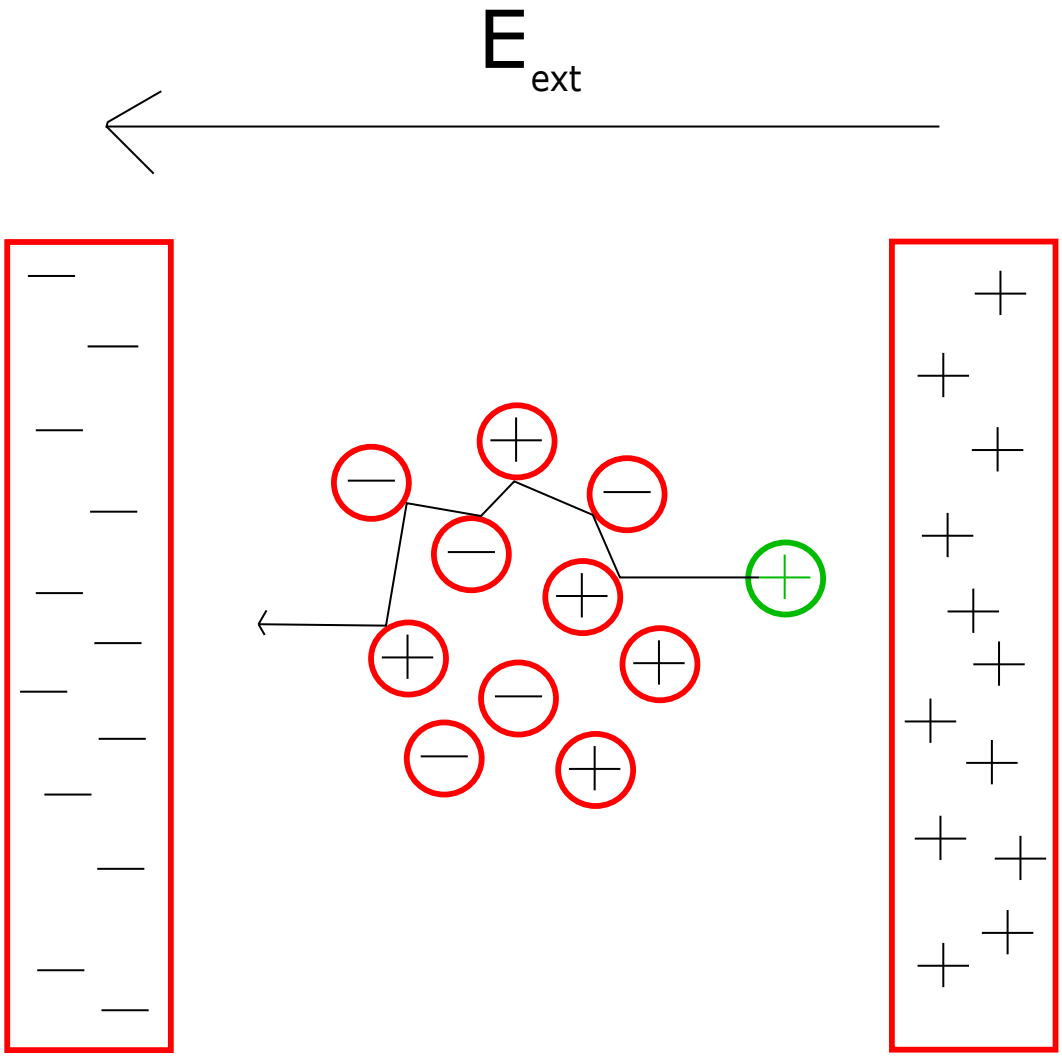

FIG. 9: Positive charge traveling in the direction of the electric field. It is inhibited by other charges in its traveling path and by the induced electric field reducing the total electric field that it experiences. Plus signs stand for positive charges and minus signs stand for negative charges.

III. EXPERIMENTAL SETUP

Our experimental setup is shown in figure 10. The light from a Ti:Sapphire laser (not shown in figure 10) is incident on a series of beamsplitters and goes through a Michelson interferometer before being focused on the contactless antenna. The first beamsplitter sends approximately 4% of the light to a photodiode that generates a clock signal used to synchronize the high voltage, high frequency power supply that provides the external electric field to the antenna. The second

beamsplitter creates a pulse with approximately 10% of the remaining energy that is used to detect and characterize the THz pulse generated by the contactless antenna. Below, we address each component of the experiment separately and in greater detail.

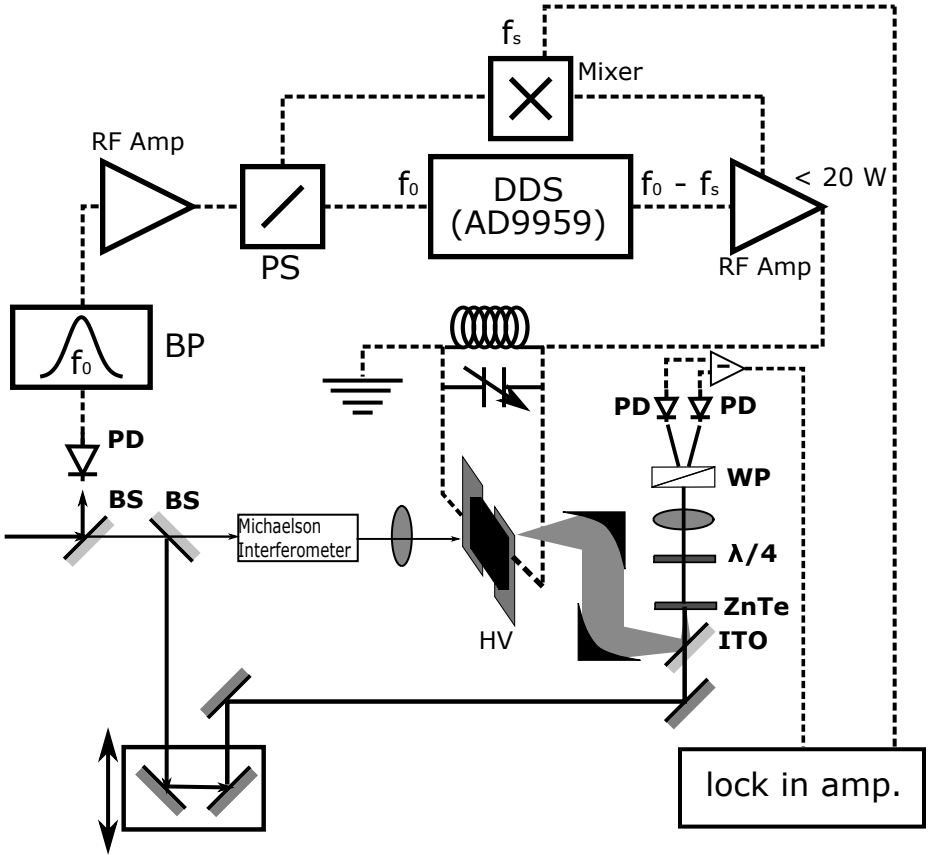

FIG. 10: Detailed schematic of experimental setup where BP stands for band-pass, PS for power splitter, BS for beam splitter, HV for high voltage, WP for Wollaston prism, PD for photodiode, ITO for indium tin oxide, and f for frequency. Showcases both electronic (upper half) and optical (lower half) modules.

A. Optical laser setup

1. Ti:Sapphire Oscillator

For this experiment, we are using a Ti:Sapphire Laser to produce broadband ultra fast laser pulses at a center wavelength of 800 nm and a frequency of 84.043 MHz. We use passive mode

locking on the laser in order to produce a pulse train rather than a continuous wave (CW) [10]. The average power of our laser is 550 mW and the per pulse energy is 6.5 nJ. The pulse duration is 30-50 fs, depending on daily alignment. Since variations in pulse duration on that order do not affect the generation of THz, we did not make careful measurements of this value.

2. Michelson Interferometer

The Michelson interferometer is a pump-probe setup that is necessary to study how the THz in the second pulse (probe) is affected by the first pulse (pump). The pump-probe method allows us to change conditions within the system and see how they affect the intensity of the THz pulse we are observing. In order for us to study saturation in THz waves, we must use the pump-probe method, where we use one pulse to excite the semiconductor in the PC antenna and the other to generate THz. As we see in Fig. 11, our laser source is split using a beam splitter into two paths. One path reflects back off a normal reflective mirror. The other path has two variables that can be adjusted. The first variable we can adjust is a neutral density filter, which attenuates the amount of power of the pump pulse. The second variable is a motorized adjustable stage which change the time delay, τ, between the pulses. Typical values in our experiment are between 1 and 3 picoseconds. Once changes have been made to the pump pulse, both pulses reach the beam splitter and overlap in the direction of the antenna.

The probe beam must be spatially aligned with the pump pulse for the pump-probe system to work, creating one beam with a two-pulse train. As stated earlier, this allows us to create changes within the pump pulse that will interact with the antenna and GaAs. Then, once the probe beam interacts with the GaAs, we can see the full effect that the pump beam had on the THz generated by the probe beam.

B. Power Supply

Our photodiode takes in the raw data of the frequency from the red pulse and sends it through a band pass filter. The filter isolates the fundamental frequency of 84.043 MHz in the pulse, which is the same frequency as the repetition rate of the Ti:Sapphire laser. We took this filtered electrical signal and amplified it to minimize the noise introduced in our power supply due to stray electronic

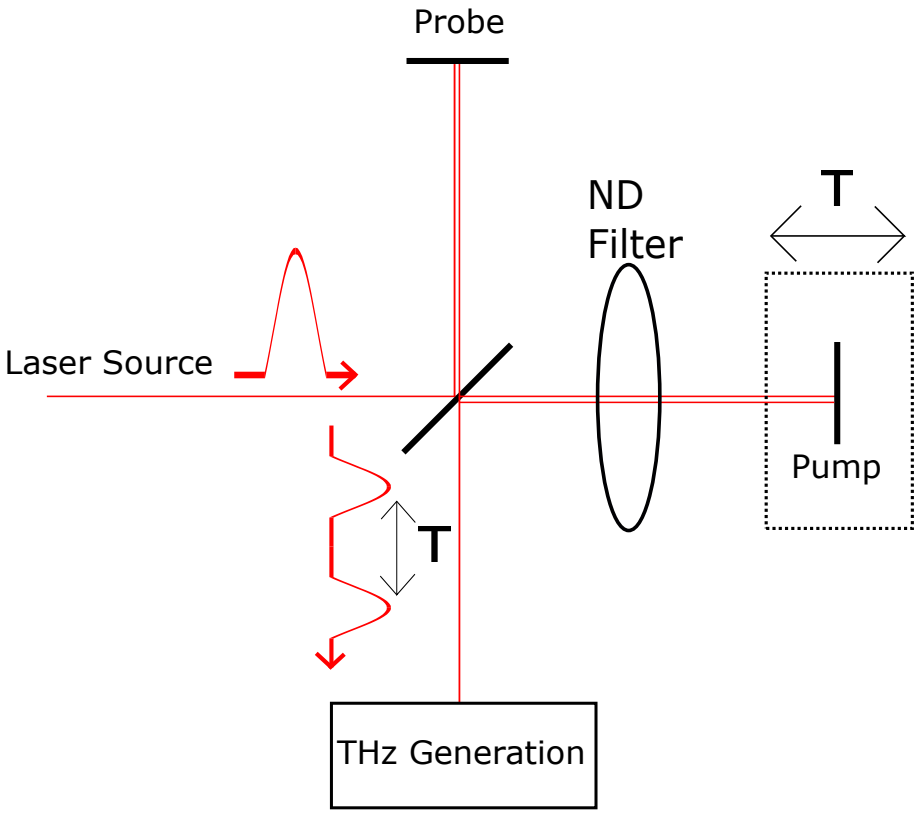

FIG. 11: Michelson Interferometer. Laser source is split at beam splitter (center) to two reflective mirrors. The probe beam is unaltered while the pump beam can be adjusted in intensity using a ND filter or position using a translation stage.

signals. That electrical signal is then split into two places, a mixer and a DDS (AD9959) board as seen in Fig. 12. The DDS board created the offset frequency of 84.033 MHz that was used in the mixer to generate the reference signal for the lock in amplifier. This offset frequency was also used in tuning the contactless antenna. This is important as the difference between the repetition rate of the laser and the offset frequency going through the high voltage antenna will assist in generating the desired THz frequency of 10 kHz. The mixer will generate a frequency that is 10 kHz based off the input of 84.043 MHz and the offset frequency of 84.033 MHz. This was used as a reference for the lock-in amplifier in order to obtain the THz signal of 10 kHz with minimal noise.

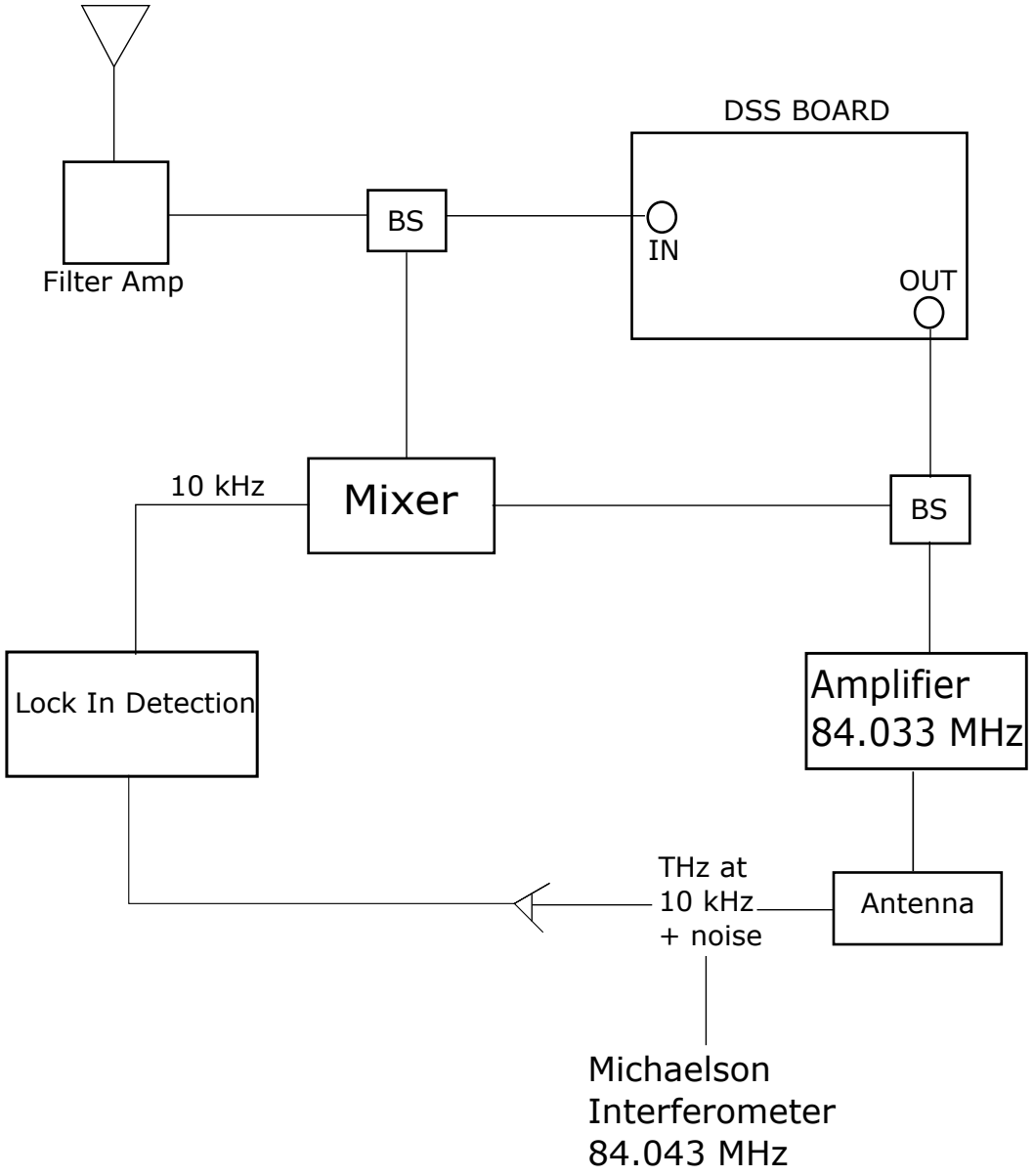

FIG. 12: Electronic portion of experimental setup. A desired frequency of 10 kHz is created for use in lock-in detection of the THz signal.

C. Detection

For detection of our THz signal, we use a common technique known as lock-in detection. This method is useful in detecting very small frequencies through highly sensitive detection. It works by taking in a clock signal, usually a modulated frequency, and Fourier filters the desired signal

around the input signal it receives. This effectively eliminates any noise that the signal has. Our lock-in detector relies on the voltage supply chain to create a reference for it to lock on to. As we stated earlier, the mixer takes the difference between the 84.043 MHz and 84.033 MHz to create a 10 kHz signal. This signal is passed into the reference port of the lock-in detector. With the reference set, the lock-in detector will take in the THz at 10 kHz with some noise, seen in Fig. 5, and lock in on the 10 kHz frequency. This will filter out unnecessary information and keep our THz signal clean.

Prior to measurements taken, the lock-in detector was phase shifted when the motor was at the position of peak THz frequency being generated (10.2mm). This maximizes our THz signal and makes analysis easier as we do not need to worry about voltage values being lost.

With the THz acting as a pump and the red pulse as a a probe, we can see how the THz affects the red pulse, using that data to visualize our THz. We used a zinc telluride (ZnTe) crystal as the medium in which our THz and red pulse laser interact. Our red probe enters the ZnTe crystal horizontally, but in the presence of THz, it's linear polarization is rotated from its initial angle of 0. This is because the THz in the ZnTe acts as an electric field, acting as a rotator, where the angle that it rotates the red beam is dependent on the strength of the THz electric field. This rotated red pulse is necessary for detection in the balanced photodiode. Before it reaches the photodiode, the rotated pulse goes through a quarter waveplate, which polarizes the beam circularly, only when there is no THz. Since the beam is rotated before the waveplate, when it hits the waveplate it becomes elliptically polarized. This is significant because in the absence of THz, the red beam travels through the ZnTe crystal linearly, therefore becoming circularly polarized, split equally by the Wollaston prism in the horizontal and vertical direction which is then detected by the photodiode as zero since it is perfectly balanced. However, if there is THz, the red beam will be rotated in the presence of THz, passing through the waveplate and becoming elliptically polarized, therefore when it reaches the Wollaston prism, the beam will not be split equally and there will be a signal coming from the degree of ellipticity. This signal is proportional to the amplitude of the THz electric field.

Before each experiment is done, we check to make sure the photodiode located after the ZnTe crystal is balanced. We check this by seeing if the voltage value it reads is close, or equal, to zero. By making sure it is zeroed, we can gather more accurate data from the THz reading as the

photodiode is dependent on the ellipticity of the polarized red pulse.

We can also think of the THz in the ZnTe crystal as a pump. The presence of THz in the crystal can rotate the polarization of a red pulse that passes through, where we can then analyze the effect on the red pulse. We then use the proportional relationship between the angle of rotation and THz intensity to record our THz signal. This form of pump- probe is integral to the detection of the THz generated.

IV. DATA AND ANALYSIS

It is important to distinguish what we mean by saturation with regards to our THz signal. If the THz signal is not saturated, we would expect to see a THz amplitude proportional to the intensity of the red pulse that creates it. However, when the THz signal is saturated, we do not see this proportionality but instead see the signal become weaker due to certain variables in the system. We can observe the changes in the second pulse in a pump probe system while keeping the properties of the Ti:Sapphire laser constant. This allow us to study how the generation of THz becomes less efficient due to saturation.

A. Saturation

In our first measurement, we test how the intensity of the pump pulse on the contactless antenna affects the amplitude of the THz electric field generated by the probe pulse. When generating our pulse with the neutral density filter, the second stage motor position was fixed, allowing for the time delay between the first and second pulse to remain constant as we adjust the neutral density filter. As we can see in Fig. 14, we see that regardless of the fluence of the first pulse, the distance between the two pulses remained the same, leading to inverse proportional changes in the max amplitude of both pulses. We subtract the data of the first pulse from the data in Fig. 14 and analyze the effect changing the fluence has on the THz in the second pulse. What we are interested in particular in Fig. 14 is the fluence of the red pulse that creates the first THz pulse, not the THz pulse itself.

In Fig. 14, we show the normalized THz amplitude of the second pulse as a function of the fluence in the first pulse. We have normalized the amplitude to the case where the fluence of the

first pulse was $0.0054 J/m^2$. For each data point, we varied the fluence of the first pulse by adjusting its intensity through an adjustable neutral density filter (as seen in 13). The fluence, in J/m^2, refers to the amount of energy deposited by the laser in a given area on the GaAs semiconductor. We can see that as we increase the intensity of the first beam, so does the fluence. In Fig. 14, we see that as the fluence increases, the THz amplitude in the second pulse decreases in a non linear fashion. This is due to Coulomb screening. With more fluence, more carriers are generated as a result in the first pulse. This is a proportional relationship, where (for example) twice the fluence in the first pulse results in twice the number of carriers generated by the first pulse.

In the period between the first and second pulse in Fig. 13 the carriers generated from the first pulse begin to thermalize meaning they are interacting with other charges in the same medium. Due to the Coulomb interactions these carriers feel, carriers begin to slow down which results in less Coulomb interactions from lack of motion. This means that the kinetic energy (KE) that these carriers had is depleted, leaving them grouped up near the center of the semiconductor. As a result, Coulomb screening is prominent by the time the second pulse arrives at the semiconductor material. We know that Coulomb screening affects the maximum THz signal generated, therefore in this case, Coulomb screening due to the first pulse will attenuate the signal generated in the second pulse. This phenomenon can be seen in our results in Fig. 13. We know that as the fluence in the first pulse increases, the THz amplitude decreases. The greater the fluence in the first pulse is, the more photogenerated carriers that are excited. With not all of the photogenerated carriers recombining before the second pulse, we get Coulomb screening, which becomes larger as more carriers populate the semiconductor. Therefor, the more fluence used, the weaker the THz signal will be due to Coulomb screening.

B. Time evolution of saturation

In Fig. 15, we show the normalized THz amplitude of the second pulse as a function of the time delay between the first and second pulse. In this experiment, we normalized the amplitude to the case where the time delay was at its largest. For each data point we shifted the motor pertaining to the first laser pulse to adjust its time delay. We saw a general relation that as the time difference between the first and second pulse increases, so does the amplitude of the THz generated in the second pulse.

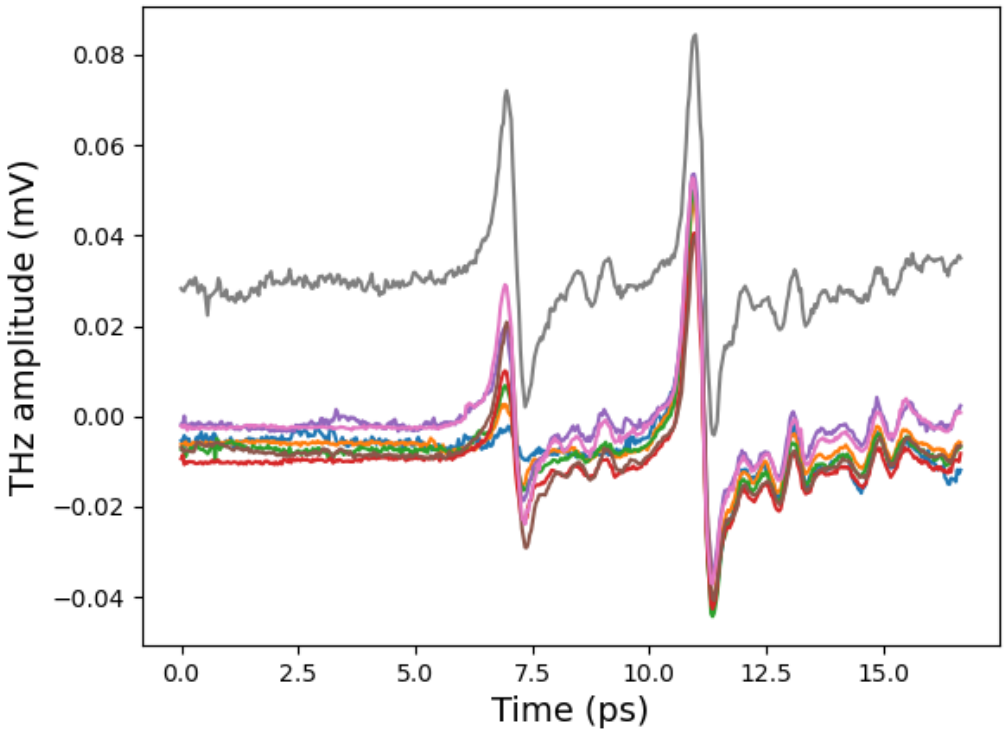

FIG. 13: Raw data of THz signal as a function of time. The time delay between the first and second pulse remain the same while the fluence in the first pulse (not shown in figure) is varied. mV stands for millivolt and ps stands for picosecond

We know that Coulomb screening in a semiconductor is stronger when the carriers existing in it have low kinetic energy. In our case, our THz signal is weaker in the presence of strong Coulomb screening. According to our data in Fig. 16, as the time delay between our pulses increases, the THz signal increases as well. The error bars were generated from two identical tests, where the time delay was the same but the amplitude of the THz was not. This means that Coulomb screening must be weakening as we increase the time delay to allow for a stronger signal. However, these results are contradictory to the results for the semiconductor InAs performed by Professor Etienne Gagnon [11]. In his study, it was shown that as time increases, the strength of the THz signal decreases. This would then show that Coulomb screening is getting larger as the time delay between pulses increases. While this data does not follow the same trend as the GaAs, we find that the time scale of both experiments leads to an explanation of this discrepancy.

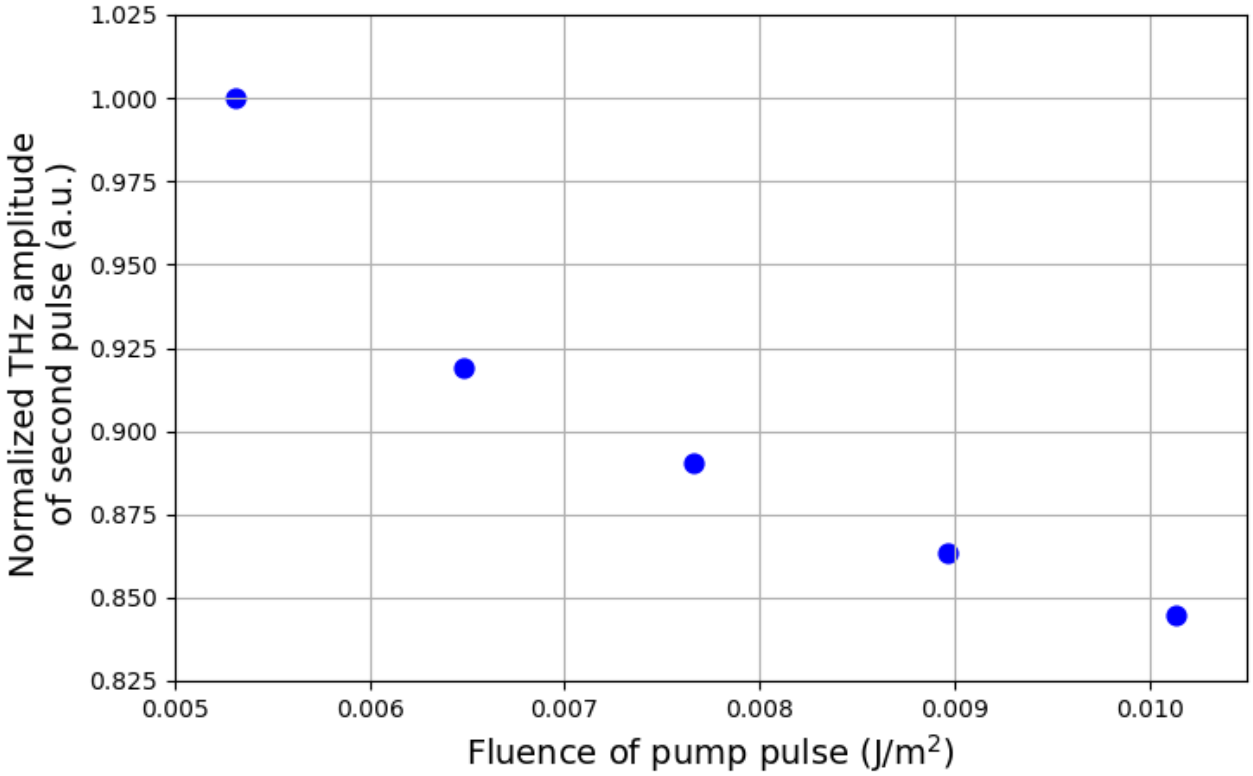

FIG. 14: Analyzed data for ND filter experiment. As the fluence of the first pulse is increased, the normalized THz amplitude begins to decrease. a. u stands for arbitrary unit, J stands for Joules and m stands for meter.

We see that the InAs data [11] that the thermalization and re-excitation of carriers have a time scale of 0-3 ps while the GaAs data has a time scale of 4-7 ps. We can see this carrier response in Fig. 17, where the InAs response has a downwards trend as time delay increases and then an non linear upward trend in the GaAs response. While we are comparing two different materials, we expect to see similar behaviors from carriers in these semiconductors. If we were to measure the timescale of thermalization in GaAs, we would find that it might differ from InAs, but the it would still follow the same general trend. For the InAs portion, the kinetic energy of the electron hole pairs generated by the first pulse decreases as the time delay between pulses increases. This is due to thermalisation and Coulomb interactions occurring in a longer period of time, decreasing the KE as a result. With the KE decreasing, Coulomb screening becomes larger, decreasing the THz

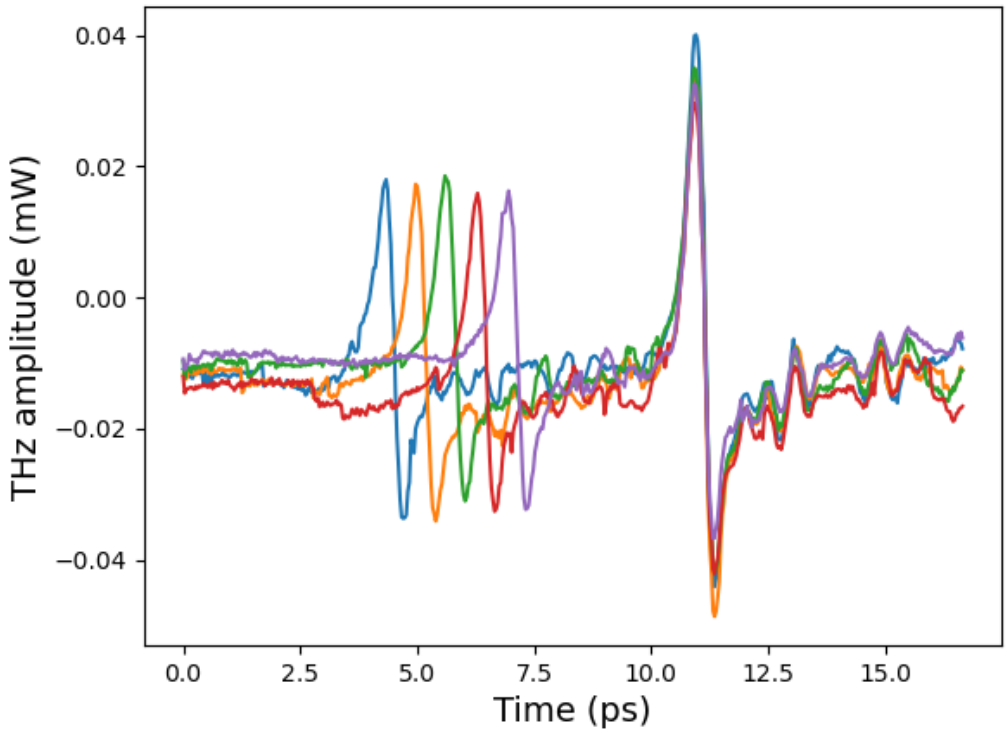

FIG. 15: Raw data of THz signal as a function of time. The time delay between the first and second pulse is varied while the fluence in the first pulse (not shown in figure) is not varied. mV stands for millivolt and ps stands for picosecond

signal. However, with the time delay increasing even further, the carriers with low KE will begin to accumulate KE due to the external field over time. This can be seen in the GaAs response in Fig. 17, where we can see as KE increases again, Coulomb screening will begin to weaken, leading to an increasing THz signal as a result.

V. CONCLUSION

In this document, we presented data showing how we can control the saturation in THz generation by adjusting the number of carriers present in the semiconductor. Using a train of two pulses, we can increase the fluence of the first pulse and see that the amplitude of the THz signal decreased. We attribute those results to Coulomb screening of the carriers generated by the second pulse and

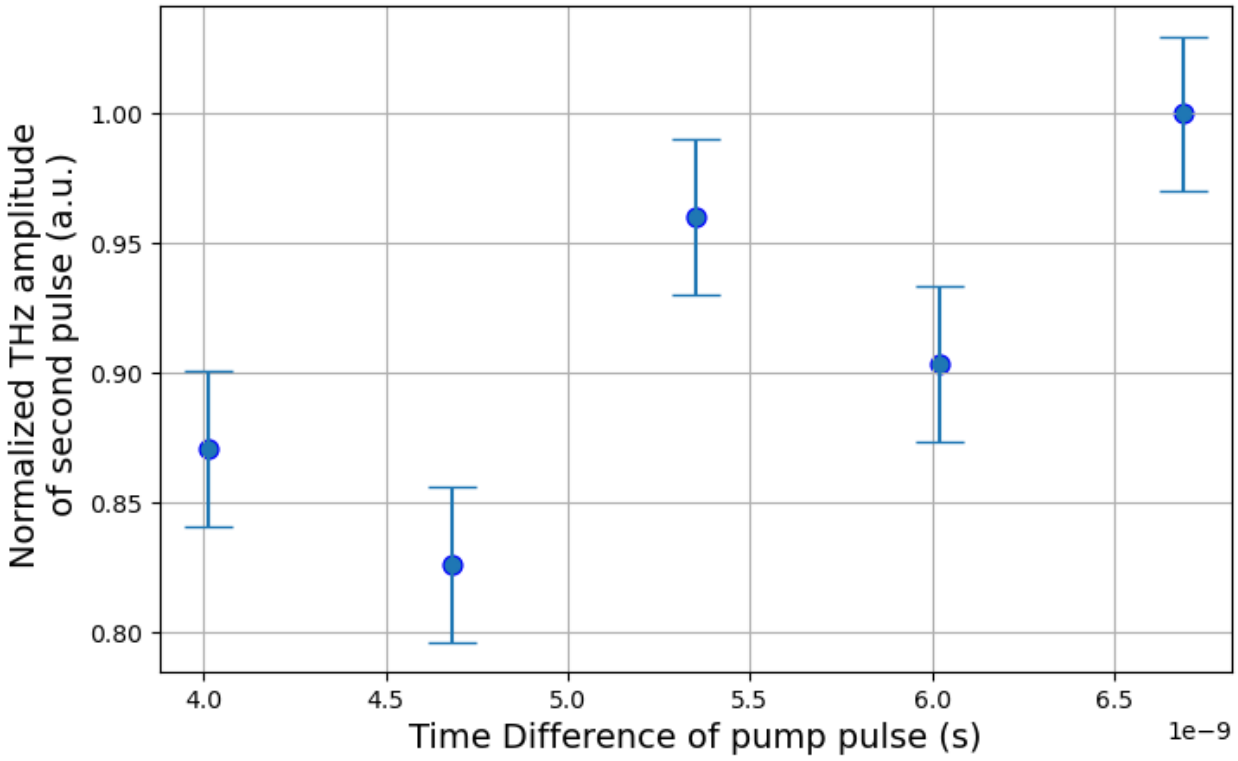

FIG. 16: Analyzed data for varied time delay between pulses. We see that as the time difference between pulses increases, the THz amplitude also increases. a. u stands for arbitrary unit and s stands for seconds.

responsible for the THz generation. We also observed how adjusting the time delay between the two pulses in the train led to an increase in the amplitude of the THz signal. This decrease in the efficiency of Coulomb screening is at first glance opposite to the results shown in the InAs data [11]. For that material, it was observed that thermalization of the carriers after photo-excitation led to more effective Coulomb screening. We can reconcile those two measurements by noticing that the timescale is different. What we observe here is the re-excitation of the carriers from the first pulse due to the external electric field after, presumably, the initial thermalization process. As the kinetic energy of the carriers increases due to re-excitation, Coulomb screening decreases and the THz signal increases. These results highlight the usefulness of using a photoconductive contactless antenna as a generation and material analysis platform.

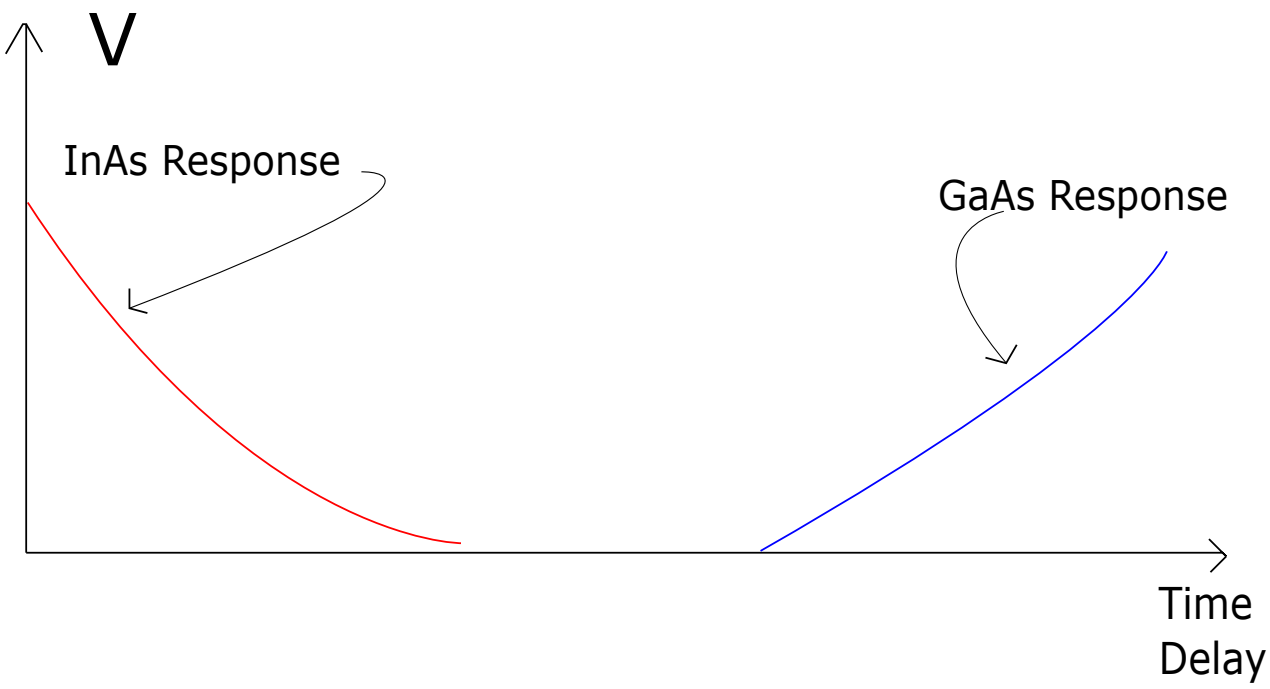

FIG. 17: Representation of InAs and GaAs voltage responses as a function of the time delay between the first pulse and second pulse. We see that in the first portion of the graph, the InAs response decreases as the time delay increases, while in the second part as the time delay increases more, the GaAs response increases. V stands for volts.

A possible future direction for this work is to find additional materials that can generate THz signals effectively. The main difficulty is to minimize the induced electric field from the motion of the intrinsic carriers by either minimizing the number of intrinsic carriers or the time they have available to move. This could be achieved by cooling our antenna or developing an even faster power supply.

VI. ACKNOWLEDGEMENTS

I would like to sincerely thank Professor Etienne Gagnon for all the mentorship and help he has provided during the development of this thesis and research. I am grateful for his guidance in navigating the experimental setup and procedures for the first time. He helped foster my newfound research skills and has truly inspired me in the field of research.

I would also like to thank Steve Spadafore with his help of developing and allowing us to use

the contactless PC antenna which was integral to the experiments we conducted.

Finally, I would like to thank the Physics and Astronomy department and Franklin and Marshall College for providing me with the resources to make all this research possible.

VII. APPENDIX

A. MATLAB Code

---

[1] K. Reimann, Reports on Progress in Physics **70**, 1597 (2007).

[2] M. O. Nathan M. Burford and El-Shenawee, Optical Engineering **56** (2017).

[3] K. S. M. Tani, S. Matsuura and S. i Nakashima, Sensors **19**, 4203 (2019).

[4] A. K. K. Z. I. O. O. C. M. N. J.-P. G. S. K. Y. K. e. a. O.A Smolyanskaya, N.V Chernomyrdin, Progress Quantum Electron **62**, 1 (2018).

[5] S. Fan, Y. He, B. S. Ung, and E. Pickwell-MacPherson, Journal of Physics D: Applied Physics **47**, 374009 (2014).

[6] X. Z. J.T Darrow and D. H. Auston, Applied Physics Letters **58**, 25 (1991).

[7] M. Reid and R. Fedosejevs, Applied Optics **44**, 149 (2005).

[8] K. S. M. Tani, S. Matsuura and S. i Nakashima, Applied Optics **36**, 7853 (1997).

[9] E. J. Galvez, *Electronics with Discrete Components* (John Wiley & Sons, Inc., 2013).

[10] P. K. D.E. Spence and W.Sibbet, OPTICS LETTERS (1991).

[11] E. Gagnon, N. K. Owusu, and A. L. Lytle, Journal of the Optical Society of America B **33**, 367 (2016).

```
st=.03; %range to generate x axis.
amp=7; %amplitude to generate induced field.  Amplitude corresponds to
       %number of intrinsic carriers in semiconductor.

range = 0:st:3*pi; %start: step(change) : end
y = 5*sin(1*range); %2*sin(9*range) %Create an external field

subplot(3,1,1);
plot(range,y,'r-') %Generating a square wave of some amplitude/frequency
subplot(3,1,2);
length(y)
g = [];
z = [];

for i = 1:length(y)
    %if i ~= length(y)
    if i == 1
        g(i) = 0; %Base Case.  Induced field is 0 at first data point of
                  %external field

    else
        g(i) = g(i-1) - amp*z(i-1)*st; %Induced field is created based off
                                       %the value of the total field.
                                       %Each consecutive data point is the
                                       %previous induced data point minus
                                       %the integral of total electric
                                       %field.
    end
    z(i) = y(i) + g(i); %Total field created through summation of a
                        %specific index of the external and induced field.
end

plot(range,g,'r-')
subplot(3,1,3)
plot(range,z,'r-')
```

FIG. 18: MATLAB code to generate Fig. 6 and Fig. 7